



Oxygen Reduction Reaction at Penta-Coordinated Co Phthalocyanines

Marco Viera¹, Jorge Riquelme¹, Carolina Aliaga¹, José F. Marco², Walter Orellana³, José H. Zagal¹ and Federico Tasca^{1*}

¹ Departamento de Química de los Materiales, Facultad de Química y Biología, Universidad de Santiago de Chile, Santiago, Chile, ² Instituto de Química Física "Rocasolano", CSIC, Madrid, Spain, ³ Departamento de Ciencias Físicas, Universidad Andrés Bello, Santiago, Chile

OPEN ACCESS

Edited by:

Wei Zhou,
Nanjing Tech University, China

Reviewed by:

Hossein Yadegari,
Imperial College London,
United Kingdom
Edson A. Ticianelli,
Universidade de São Paulo São
Carlos, Brazil

*Correspondence:

Federico Tasca
federico.tasca@usach.cl

Specialty section:

This article was submitted to
Electrochemistry,
a section of the journal
Frontiers in Chemistry

Received: 25 October 2019

Accepted: 09 January 2020

Published: 29 January 2020

Citation:

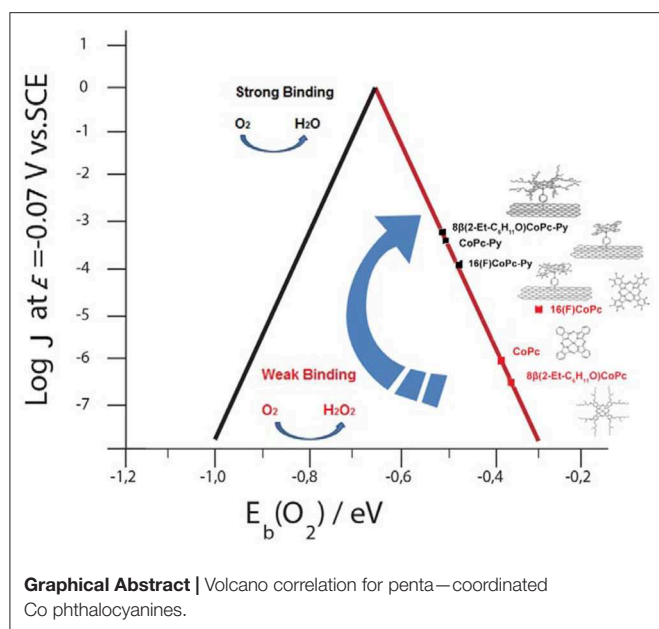
Viera M, Riquelme J, Aliaga C,
Marco JF, Orellana W, Zagal JH and
Tasca F (2020) Oxygen Reduction
Reaction at Penta-Coordinated Co
Phthalocyanines. *Front. Chem.* 8:22.
doi: 10.3389/fchem.2020.00022

From the early 60s, Co complexes, especially Co phthalocyanines (CoPc) have been extensively studied as electrocatalysts for the oxygen reduction reaction (ORR). Generally, they promote the 2-electron reduction of O₂ to give peroxide whereas the 4-electron reduction is preferred for fuel cell applications. Still, Co complexes are of interest because depending on the chemical environment of the Co metal centers either promote the 2-electron transfer process or the 4-electron transfer. In this study, we synthesized 3 different Co catalysts where Co is coordinated to 5 N atoms using CoN₄ phthalocyanines with a pyridine axial linker anchored to carbon nanotubes. We tested complexes with electro-withdrawing or electro-donating residues on the N₄ phthalocyanine ligand. The catalysts were characterized by EPR and XPS spectroscopy. Ab initio calculations, Koutecky–Levich extrapolation and Tafel plots confirm that the pyridine back ligand increases the Co–O₂ binding energy, and therefore promotes the 4-electron reduction of O₂. But the presence of electron withdrawing residues, in the plane of the tetra N atoms coordinating the Co, does not further increase the activity of the compounds because of pull-push electronic effects.

Keywords: Co phthalocyanine, penta-coordinated Co phthalocyanines, oxygen reduction reaction, electrocatalysis, volcano correlations

INTRODUCTION

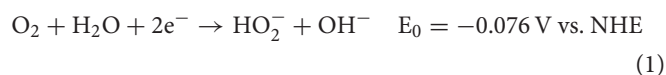
Metal phthalocyanines and porphyrins (MPc) belong to the category of macrocyclic complexes where a metallic redox center is coordinated by four pyrrolic nitrogen atoms (MN₄). Because of the interesting physical and chemical properties and of the similarities of those molecules to other catalysts found in nature, MN₄ have been broadly studied since the early 1960s. In particular, Co phthalocyanine (CoPc) was reported to be an electrocatalysts for the oxygen reduction reaction (ORR) by Jasinski (1964). Later the activity of those complexes was studied for other important reaction like the CO₂ reduction (Morlanes et al., 2016; Zhang et al., 2017), and the oxidation of L-cysteine (Gulppi et al., 2014), hydrazine (Geraldo et al., 2002, 2008; Venegasa et al., 2017), thiocyanate (Linares-Flores et al., 2012) and thiols (Bedioui et al., 2007) and also for their bio-mimicking activity (Zagal et al., 2010; Venegas et al., 2017; Herrera et al., 2018; Riquelme et al., 2018a).



The search for electrocatalysts for the ORR as active and durable as the rare and costly Pt (which is the industrial standard for this reaction) is still pushing the search for a non-precious metal catalyst. The difficulties at finding an appropriate catalyst arise from the complexity of the reaction the lower activity and stability. From the moment that up to 4 electrons and 4 protons are necessary for the complete reduction of dioxygen various intermediates can be formed during the process accounting for the so-called “scaling relationship” (Nørskov et al., 2004; Koper, 2011; Christensen et al., 2016; Katsounaros and Koper, 2017).

For example, in alkaline media, the reaction might proceed via a 2-electron transfer process (following reaction 1) with the release of HO_2^- or via a 4-electron transfer (following reaction 2) leading to formation of H_2O with the splitting of the O-O bond.

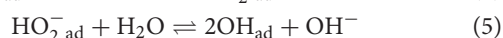
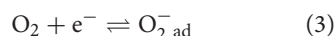
2-electron transfer ORR in basic media:



4-electron transfer ORR in basic media:



For the 4-electron transfer process the intermediates are:



Depending on the pathway of the reaction we might have 2 or 3 intermediates bound to the active sites as $\text{O}_2^- \text{ad}$, $\text{HO}_2^- \text{ad}$ and OH_{ad} or dissolved HO_2^- if the reaction proceeds as in Equation (1).

The ORR catalyzed at electrodes modified with CoN4 complexes is of major interest because of the ease and the convenience of the synthesis of those redox complexes and because of the different catalytic properties of the various complexes which were synthesized to optimize the catalysis. For example ORR catalyzed by unsubstituted CoPc or by CoPc with the addition of one or more electron-donating or electron-withdrawing substituents adsorbed directly on graphite proceeds via a 2-electron transfer process (Zagal et al., 1992; Sun et al., 2014; Zagal and Koper, 2016; Ye et al., 2017; Abarca et al., 2019) whereas complexes with pendant residues that increase the electron back-bonding would promote a direct 4-e process as in Equation (2) (Steiger and Anson, 1995; Tse et al., 1997; Riquelme et al., 2018a,b). Co-cofacial bimetallic complexes and dimeric Co porphyrins that bind simultaneously both dioxygen atoms would also transfer directly 4 electrons to O_2 (Collman et al., 1980; Durand et al., 1983; Le Mest et al., 1997; Peljo et al., 2012; Swavey and Eder, 2013; Wada et al., 2013; Dey et al., 2017; Oldacre et al., 2018). Penta-coordinated complexes involve a Co center coordinated to 4 planar N atoms and an axial N belonging to a pyridine molecule as for example in VB12 seem to promote a 4-e process. CoPc-Py-CNT complex also promotes the reduction of dioxygen following a mixed 2 and 4-electrons process (Zagal et al., 2010; Fukuzumi et al., 2018; Riquelme et al., 2018a; Zhou et al., 2019). Recently, Zhou and collaborators studied the effect of various axial ligands on the activity of Co porphyrin toward the ORR (Zhou et al., 2019). They found that an increased coordination strength of the axial ligand leads to higher activity of the catalyst (Zhou et al., 2019). Because of the presence of the fifth coordination the d orbitals of the Co redox center would become more similar to the orbitals of O_2 and therefore Co would form a stronger bond with O_2 . It is important to point out that in correlations of activity vs. the M- O_2 binding energy, volcano correlations are obtained using a great number of MN4 complexes of Cr, Mn, Fe, Co, and Cu as central metals. Strongly O_2 binding complexes lie on one side of the volcano and weakly binding complexes lie on the other side of the volcano. Most CoN4 complexes, including CoPc appear on the weak binding side. This indicates that the activity of these CoN4 catalysts increases as the Co- O_2 binding energy increases. It was shown for planar CoN4 complexes, that stronger electron withdrawing planar residues would reduce the distance between the O_2 and Co orbitals increasing as the Co- O_2 binding energy (Van Den Brink et al., 1983; Zagal et al., 1992).

What happens in the presence of fifth axial coordination? How does the fifth coordinated N affect the Co- O_2 binding energy of CoN4? How does it affect the activity of CoN4 complexes toward the ORR when in the presence of ligands in the plane of the phthalocyanine ring? Can a linear correlation be reproduced as for the planar catalysts?

To answer those questions unsubstituted CoPc, perfluorinated CoPc (16(F)CoPc), and Cobalt-octaethylhexyloxyphthalocyanine (8(2-Et-C₆H₁₁O)CoPc) were coordinated to CNT modified with covalently attached pyridine moieties. Their activities at modified rotating ring disk electrodes were compared to that of the planar catalysts physically adsorbed on unmodified CNT. EPR and XPS spectroscopy analysis confirm the changes of the electronic

structure of the Co redox center while DFT calculations provide the O₂-Co binding energy of the complexes. Stronger Co-O₂ binding energy leads to higher ORR catalytic activity.

EXPERIMENTAL

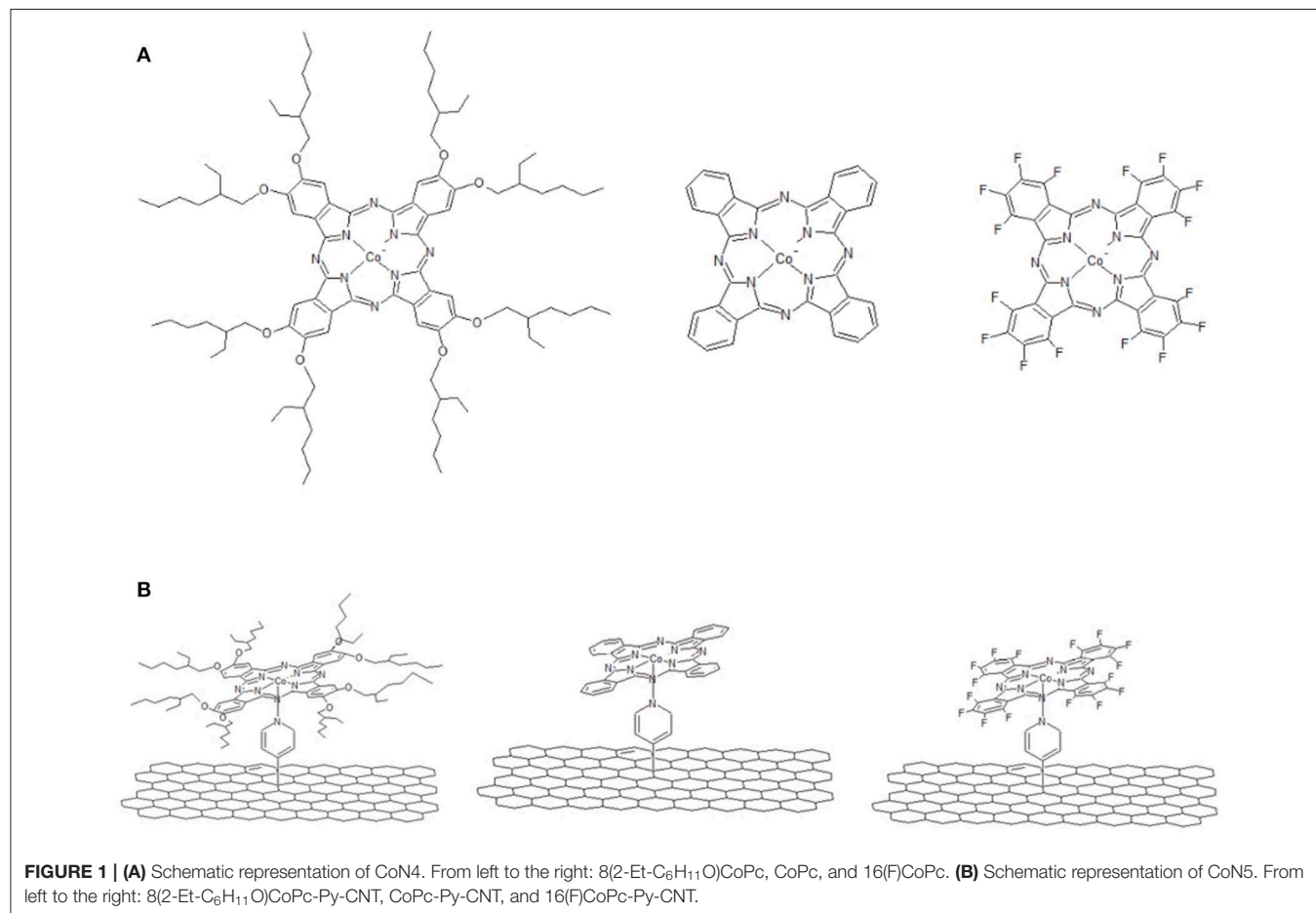
Modification of Co Phthalocyanines

Cobalt phthalocyanine (CoPc), cobalt-hexadecafluorophthalocyanine (16(F)CoPc), and 4-aminopyridine (Py), 2,2-diphenyl-1-picryl-hydrazyl (DPPH), N,N-dimethylformamide (DMF), isopropyl alcohol, NaOH, HCl, K₂HPO₄ were obtained from Sigma (St. Louis, USA). Cobalt-octaethylhexyloxyphthalocyanine (8(2-Et-C₆H₁₁O)CoPc), was synthesized according to the literature (Weber and Busch, 1965). CNT were from Nanocyl (Sambreville, Belgium). Previously to modification the CNT were The functionalization of the CNT with Py was obtained using the diazonium reaction where 0.1 g of CNT dispersion was added to 5 g of NaNO₂, 7 g of Py, and 1 g of DPPH 5 ml of 4 M HCl water solution; DPPH was used as radical scavenger to prevent the formation of multi-layers (Menanteau et al., 2016). The Py-CNT were washed with isopropanol and water, filtered and dried in a furnace at 80°C. Next, the Py-CNT were suspended in DMF and modified with either CoPc, or with 16(F)CoPc,

or with 8(2-Et-C₆H₁₁O)CoPc by refluxing in N₂ at 150°C to obtain CoPc-Py-CNT, 16(F)CoPc-Py-CNT, and 8(2-Et-C₆H₁₁O)CoPc-Py-CNT. To modify electrodes an ink of the modified phthalocyanine was obtained by dispersing 1 mg of the complex in 1 ml of a mixture of 25% volume isopropyl alcohol and 75% H₂O. Finally, 20 μl of ink (final load 0.1 mg cm⁻²) was dropped onto the surface of the electrode and let to dry.

Electrochemical Characterization

Orignalys (Rillieux-la-Pape, France) KCl saturated Ag|AgCl was used as reference electrode and all the potentials are reported using this reference. As working electrode, a rotating ring disk electrode (RRDE) from Pine Instruments (Durham, NC, USA) was used. An edge-plane pyrolytic graphite disk (5 mm diameter and 4 mm thick), was mounted into a Teflon rotating shaft containing the Pt ring electrode (external diameter of 7.50 mm, internal diameter 6.50 mm). The MSR rotator was also from Pine Instruments (Durham, NC, USA). 800 grit emery paper was used to renew the graphite disk. An Autolab PGSTAT 302N with a dual mode bipotentiostat module (Utrecht, The Netherlands) was used to perform electrochemical experiments. During linear sweep voltammetry experiments the ring potential was set to 0.65 V vs. Ag|AgCl.

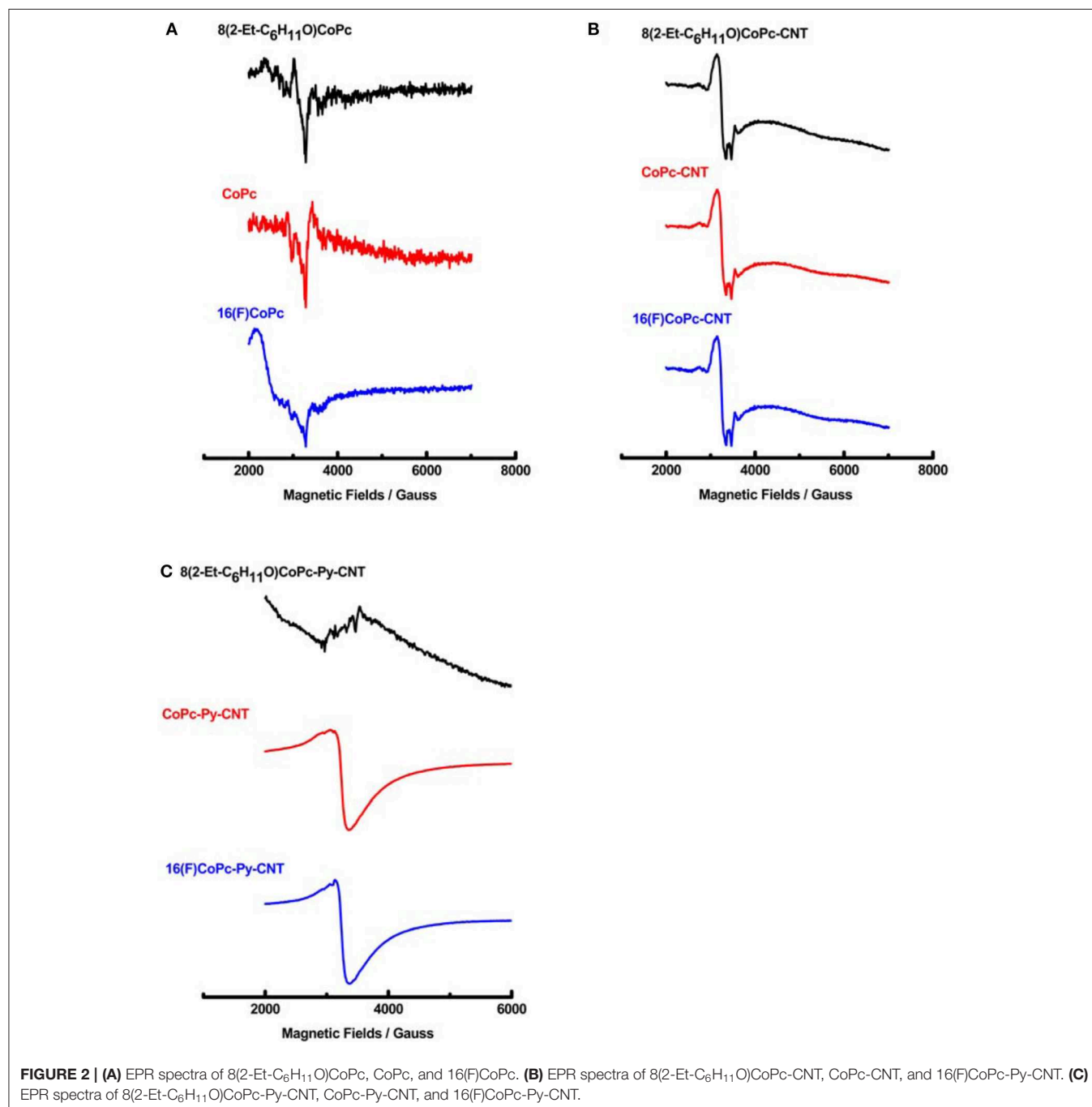


EPR and XPS Spectroscopy

Dried powder CNT and of each pure and modified complex was used for EPR and XPS spectra. EPR spectra were collected at 298 K with a Bruker EMX-1572 spectrometer working at 9.39 GHz (X-band), using powder samples. XPS spectra were recorded at the Recasolano center using a vacuum of ca. 3×10^{-9} mbar, a PHOIBOS-150 electron analyzer (SPECS), Al K α radiation (1486.6 eV, 100 W) and constant pass energy of 20 eV. The binding energy scale was referenced at the main C 1s signal, which was set at 284.6 eV.

Theoretical *ab-initio* Calculations

The Quantum-ESPRESSO *ab initio* package was used to perform spin-polarized density functional theory (DFT) calculations (Giannozzi et al., 2009). Dispersive interactions were included by the van der Waals functional (vdW-DF2) into the exchange-correlation potential (Berland et al., 2015). Kohn-Sham eigenfunctions were expanded on a plane-waves basis set where the interaction between valence electrons and ion cores were described by ultrasoft pseudo-potentials (Garrity et al., 2014). Converged results have been achieved by using cut-off energies



of 35 Ry on plane waves and of 280 Ry on the electronic density. We consider an (8,8) single-walled carbon nanotube (CNT) with 11 Å in diameter. Calculations were conducted in large unit cells with periodic boundary conditions along the CNT axis, including a vacuum region of 15 Å. The sampling in the irreducible part of the Brillouin zone was restricted to the Γ point. The systems were fully relaxed until the force in each atom component was <0.025 eV/Å. The activation energy for the O₂ dissociation was obtained by calculating the minimum energy path using the Nudged Elastic Band (NEB) method (Henkelman et al., 2000), considering 10 images in the reaction coordinate.

RESULTS AND DISCUSSION

In **Figure 1** we report a schematic representation of CoPc, 16(F)CoPc and 8(2-Et-C₆H₁₁O)CoPc molecules (**Figure 1A**) and the corresponding molecule coordinated to the pyridine modified CNT (i.e., CoN4-Py-CNT) (**Figure 1B**). The modification of CNTs with pyridine moieties to form Py-CNT has been reported previously (Bahr and Tour, 2001; Tasca et al., 2011; Tuci et al., 2014; Venegas et al., 2017; Riquelme et al., 2018a). Also, the modification of CoN4 with pyridine or similar strongly

coordinating solvents has been shown before (Cariati et al., 1975; Liao and Scheiner, 2001; Riquelme et al., 2018a). Nevertheless, the synthesis and the studies of the ORR at substituted penta-coordinated CoPc have not been reported before.

EPR and XPS Characterization

To obtain insights into the redox state and the spin state of the d electron in CoN4 and CoN5 complexes, EPR and XPS spectra of the complexes were obtained. The EPR spectra of 8(2-Et-C₆H₁₁O)CoPc, CoPc, and 16(F)CoPc molecules do not present strong EPR signals at room temperature but only features at around 2000 G corresponding to the presence of the low spin form of Co(II) (**Figure 2A**). Co phthalocyanines EPR spectra were previously studied in details by Assour (1965), and Kontarinis et al. (2003). The EPR spectrum of the complexes in the presence of CNT, are shown in **Figure 2B**. CNT powder has a strong signal due to defects in the graphene structure (Corzilius et al., 2007; Riquelme et al., 2018a) with a g factor value of 2.055 (Riquelme et al., 2018a). The signal of CNT modified with the various Co phthalocyanines, varies in each sample (**Figure 2B**), indicating the electronic interaction between the CNT and the adsorbed moieties. When in the presence of the pyridine modified CNT, the g factor value of the CoN5 complexes drastically decreases because of the new chemical environment with the exception of sample 8(2-Et-C₆H₁₁O)CoPc-Py-CNT where no EPR signal is observed because of a high spin ($S = 3/2$) Co(II) specie (**Figure 2C**). The EPR spectrum of the penta-coordinated compounds CoPc-Py-CNT and 16(F)CoPc-Py-CNT presents a value of g_{iso} around 2.08 consistent with a Co(III) in a low spin state (LS) $S = 1/2$, where the electron is occupying a d_{z^2} type orbital or a Co(II) in a low spin configuration $S = 1/2$. The hyperfine structures were not observed at room temperature (Baumgarten et al., 2001).

The interpretation of the Co 2p XPS data in systems like these is not straightforward. Low spin ($S = 0$) diamagnetic Co(III) and high spin ($S = 3/2$) paramagnetic Co(II) compounds show very characteristic spectra (Briggs and Gibson, 1974; Frost et al., 1974; Oku, 1978). In the case of low spin ($S = 1/2$) Co(II) complexes, the Co 2p spectra show very subtle differences with respect to the spectra pertaining to low spin ($S = 0$) Co(III) and care must be taken when carrying out the corresponding analysis. The less usual intermediate spin ($S = 1$) Co(III) complexes have also very distinctive features (Oku, 1978). The binding energies of the main photoemission lines is not always indicative of the oxidation state or the changes in charge distribution of cobalt since they can be affected by the type of ligands or the spin state (Briggs and Gibson, 1974). Therefore, it is better to resort to other spectral features as the presence or absence of shake-up satellite structure (which inform on the paramagnetic or diamagnetic nature, respectively, of the cobalt ion), the occurrence of multiplet splitting and the energy separation, ΔE , between the Co 2p_{3/2} and Co 2p_{1/2} core level lines. Thus, low spin ($S = 0$) diamagnetic Co(III) complexes show Co 2p spectra with narrow, quite symmetric lines, the absence of multiplet splitting peaks because Co(III) ($S = 0$) has no unpaired electrons, almost total absence of satellites except for a weak one (interpreted as an energy loss feature) at about 10 eV above the main Co 2p_{3/2} line and

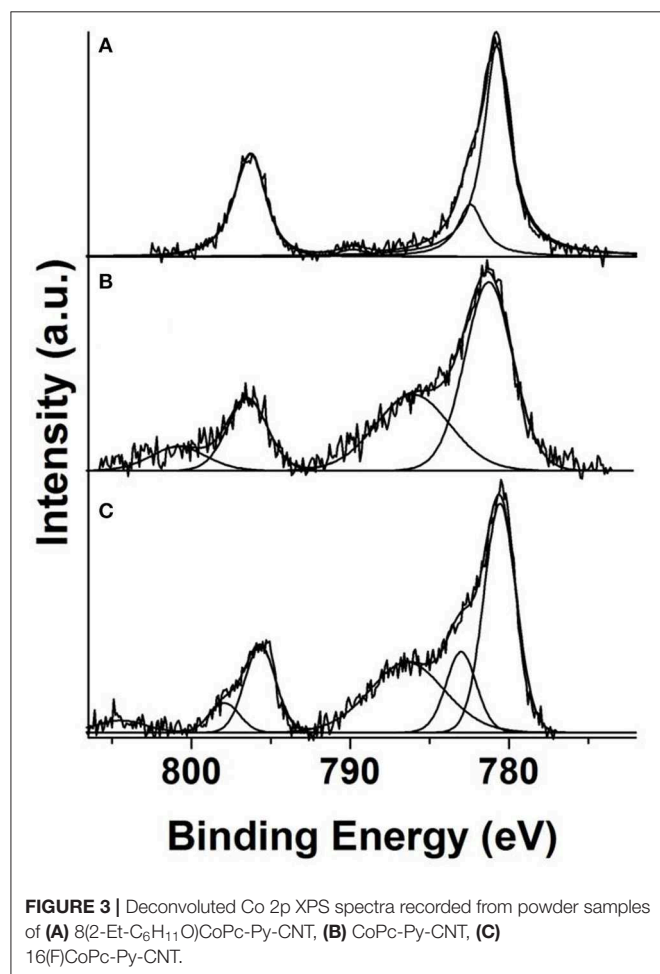


FIGURE 3 | Deconvoluted Co 2p XPS spectra recorded from powder samples of (A) 8(2-Et-C₆H₁₁O)CoPc-Py-CNT, (B) CoPc-Py-CNT, (C) 16(F)CoPc-Py-CNT.

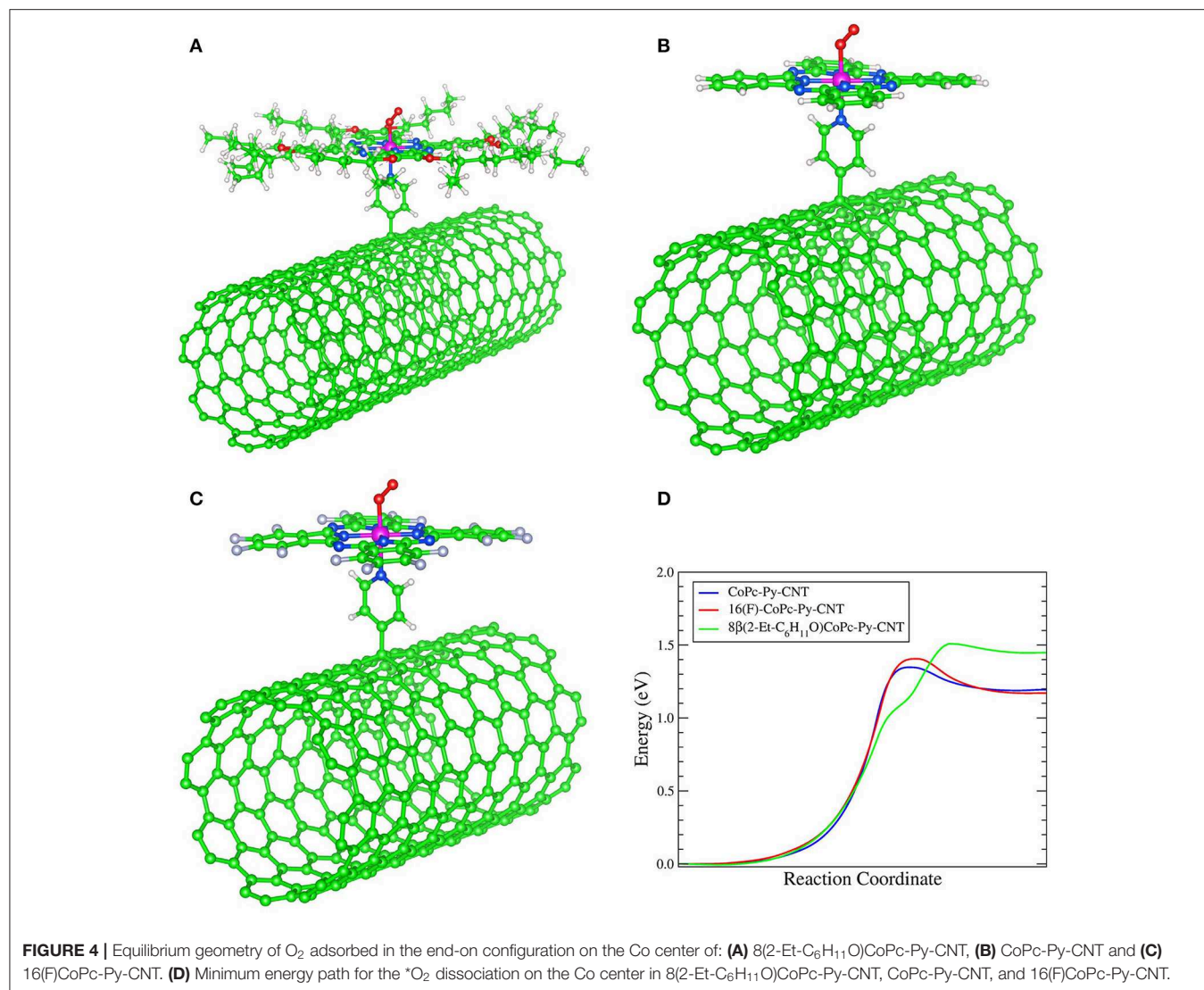


TABLE 1 | Resume of the total energy for 8(2-Et-C₆H₁₁O)CoPc-Py-CNT, CoPc-Py-CNT, and 16(F)-CoPc-Py-CNT with and without the O₂ molecule adsorbed on the Co metal center for the allowed spin states.

<i>m</i> (μB)	8β(2-Et-C ₆ H ₁₁ O)CoPc-Py-CNT	O ₂ -8β(2-Et-C ₆ H ₁₁ O)CoPc-Py-CNT	CoPc-Py-CNT	O ₂ -CoPc-Py-CNT	16(F)-CoPc-Py-CNT	O ₂ -16(F)CoPc-Py-CNT
	<i>E</i> _{total} (eV)	<i>E</i> _{total} (eV)	<i>E</i> _{total} (eV)	<i>E</i> _{total} (eV)	<i>E</i> _{total} (eV)	<i>E</i> _{total} (eV)
0	E ₀ + 0.06	E ₀ + 0.04	E ₀ + 0.06	E ₀ + 0.08	E ₀ + 0.05	E ₀ + 0.04
1	E ₀	E ₀ + 0.08	E ₀	E ₀	E ₀	E ₀ + 0.09
2	E ₀ + 0.03	E ₀	E ₀ + 0.04	E ₀ + 0.04	E ₀ + 0.04	E ₀
3	E ₀ + 0.10	E ₀ + 0.09	E ₀ + 0.15	E ₀ + 0.13	E ₀ + 0.15	E ₀ + 0.11

a $\Delta E = 15.0\text{--}15.1\text{ eV}$ (Briggs and Gibson, 1974; Frost et al., 1974; Oku, 1978). On the contrary, paramagnetic ($S = 3/2$) high spin Co(II) ions present Co 2p spectra with broad and asymmetric lines due to the occurrence of multiplet splitting, intense shake-up satellite structure ca. 5.6–6.0 eV above the main Co 2p_{3/2} line and a $\Delta E = 16.0\text{ eV}$ (Briggs and Gibson, 1974;

Frost et al., 1974). The Co 2p spectra of intermediate spin ($S = 1$) Co (III) complexes may have asymmetric lines because of multiplet splitting, satellites at about 3.2–4.2 eV above the main Co 2p_{3/2} photoemission line and a ΔE intermediate between 15.0 and 16.0 eV (Oku, 1978). Finally, low spin ($S = 1/2$) Co(II) complexes give Co 2p spectra with very weak satellites but having

multiplet splitting peaks about 2.0 eV above the main Co 2p_{3/2} line which are displayed as a shoulder or asymmetry of that peak. For these compounds, the value of ΔE is also intermediate between 15.0 and 16.0 eV (Briggs and Gibson, 1974; Frost et al., 1974). An interesting observation is that in low spin ($S = 1/2$) Co(II) multiplet splitting peaks are observed mainly close to the Co 2p_{3/2} peak, but are less evident, or simply inexistent, close to the Co 2p_{1/2} peak (Briggs and Gibson, 1974). However, shake up satellites appear on the high binding energy side of both photoemission lines.

Having all this information in mind we can face now the interpretation of the Co 2p spectra recorded from 8(2-Et-C₆H₁₁O)CoPc-Py-CNT, CoPc-Py-CNT, and 16(F)CoPc-Py-CNT and which are shown in **Figures 3A–C**, respectively. The spectrum recorded from CoPc-Py-CNT shows a relatively narrow doublet with a binding energy of the Co 2p_{3/2} core level of 780.8 eV and $\Delta E = 15.5$ eV. The Co 2p_{3/2} line is clearly asymmetric in its high binding energy side having a clear shoulder at 782.3 eV, i.e., 1.7 eV above the binding energy of the mentioned line. This shoulder, as stated above, is compatible with the occurrence of multiplet splitting and, therefore, compatible with a low spin ($S = 1/2$) Co(II) species. The Co 2p spectrum recorded from 16(F)CoPc-Py-CNT is very different. It shows much broader lines and the presence of very intense shoulders above the main photoemission lines. Since these shoulders appear close to both core level lines they must correspond with shake-up satellites. The Co 2p_{3/2} peak is located at 781.2 eV ($\Delta E = 15.3$ eV) and its corresponding satellite at 785.4 eV, i.e., a separation of 4.2 eV. All these values support the assignment of this spectrum to an intermediate spin ($S = 1$) Co(III) species. Finally, the Co 2p spectrum recorded from 8(2-Et-C₆H₁₁O)CoPc-Py-CNT is also different from the spectra recorded from the other two samples. In this spectrum the photoemission lines are clearly asymmetric having shoulders in their high binding energy side (~ 2.4 eV) what is indicative of the occurrence of multiplet splitting. The spectrum also shows the presence of a clear and intense shake-up satellite at 786.5 eV, i.e., 6.0 eV above the main Co 2p_{3/2} peak which is located at 780.5 eV. All this allows, with no doubt, to identify the Co ion in this compound as a high spin ($S = 3/2$) Co(II) species.

DFT Calculations

We performed spin-polarized DFT calculations to simulate the structure of the CoN5, the binding energy of O₂ to Co redox centers, and the activation energy for the ORR. In **Figures 4A–C** we show the stable geometries of the O₂ molecule adsorbed on the Co metal center of 8(2-Et-C₆H₁₁O)CoPc-Py-CNT, CoPc-Py-CNT, and 16(F)CoPc-Py-CNT. For the three complexes, O₂ is found to bind in the end-on configuration. The total energy was calculated for the allowed spin state in order to find the most stable spin configuration. Our results show that all the complexes in their equilibrium geometry exhibit a low-spin configuration, showing a magnetic moment $m = 1 \mu_B$, that is with an unpaired electron ($S = 1/2$). After approaching at the CoN5 center, the O₂ molecule attaches to the Co atom with one O atom with binding energies of -0.595 , -0.532 , and -0.524 eV for

CoPc-Py-CNT, 16(F)CoPc-Py-CNT, and 8(2-Et-C₆H₁₁O)CoPc-Py-CNT, respectively. Interestingly, the equilibrium spin state of the complexes with the adsorbed O₂ molecule shows different spin configurations with $m = 1 \mu_B$ for CoPc-Py-CNT and $m = 2 \mu_B$ for 16(F)CoPc-Py-CNT, and 8(2-Et-C₆H₁₁O)CoPc-Py-CNT. In **Table 1** we report the equilibrium geometry of O₂ attached to the Co center for the three compounds. We observe that for O₂-CoPc-Py-CNT, the O-Co bond distances are shorter than those found in O₂-16(F)CoPc-Py-CNT and O₂-8(2-Et-C₆H₁₁O)CoPc-Py-CNT, which indicate that the CoPc border modifications tend to weaken the O₂-Co bond, consistent with the smaller O₂ binding energy, as reported in **Table 2**. Moreover, the distance between the Co atom and the N axial ligand [N(a)-Co] in O₂-CoPc-Py-CNT is shorter than in the other compounds. This suggests a higher electronic localization at the Co center, which may explain the higher magnetic moment observed in O₂-CoPc-Py-CNT. We also studied the activation energy for the O₂ dissociation after adsorption on the Co center by calculating the minimum energy path of the reaction using the NEB method. **Figure 4D** shows the results for the three complexes. The calculated activation energies (the height of the barriers) range between 1.35 to 1.51 eV, where CoPc-Py-CNT would show the lowest value, close to 16(F)CoPc-Py-CNT. If we associate lower activation energy with higher catalytic activity, the ORR catalytic activity for the complexes under study would follow the trend CoPc-Py-CNT \geq 16(F)CoPc-Py-CNT > 8(2-Et-C₆H₁₁O)CoPc-Py-CNT. Anyway, the activities of the three compounds do not vary much. **Table 2** compares our results for O₂ binding and activation energies for the three complexes. We observe a clear correlation between higher O₂ binding energies with lower O₂ activation energies, where better ORR catalyst would attach O₂ with binding energies close to -0.6 eV. We also calculated the O₂ interaction on the Pt(111) surface, which is the industrial standard catalyst for the ORR. We find O₂ binding energy of -0.65 eV and activation energy of 1.0 eV, which are close to those found for O₂ on CoN5. To the best of our knowledge, this is the first time that Eb(O₂) is calculated for CoN5 catalysts out of CoPc-Py-CNT and VB12 (Riquelme et al., 2018a). Eb(O₂) is generally used as reactivity index in heterogeneous catalysis as well as in electrocatalysis. For example Norskov et al. reported volcano plot of activities (J, current density) of metal catalysts vs. Eb(OH) and suggested that in

TABLE 2 | Theoretical results for the magnetic moment (m), O₂ binding energy (E_{bind}), and O₂ activation energy (E_{activ}) for 8(2-Et-C₆H₁₁O)CoPc-Py-CNT, CoPc-Py-CNT, 16(F)-CoPc-Py-CNT, 8(2-Et-C₆H₁₁O), CoPc, and 16(F)CoPc in their lowest energy state.

Compound	m (μ_B)	O ₂ E_{bind} (eV)	O ₂ E_{activ} (eV)
8 β (2-Et-C ₆ H ₁₁ O)CoPc-Py-CNT	1	-0.524	1.51
CoPc-Py-CNT	1	-0.593	1.35
16(F)CoPc-Py-CNT	1	-0.532	1.41
8 β (2-Et-C ₆ H ₁₁ O)CoPc	1	-0.346	
CoPc	1	-0.382	
16(F)CoPc	1	-0.324	

one side of the volcano we would find strong binding site vs. the opposite side of the volcano where weak binding site would occur or in other words 4-electron catalysts as Pt in one side vs. 2-electron catalysts as Au or Ag at the other side of the plot (i.e., the weak binding side of the volcano; Viswanathan et al., 2012; Hansen et al., 2014). Zagal and Koper reported similar plots for MN₄ complexes, distinguishing FeN₄ and MnN₄ as strong O₂ binders while CoN₄ and NiN₄ would interact with O₂ too weakly (Zagal and Koper, 2016). We recalculated the $E_b(O_2)$ for 8(2-Et-C₆H₁₁O)CoPc, CoPc, and 16(F)CoPc, and we found values that range between -0.32 eV to -0.38 eV (values resumed in **Table 2**). The performed calculations well agree with the previously estimated value of MN₄ (Ruiz-Tagle and Orellana, 2010; Orellana, 2012, 2013). CoN₅ would then bind O₂ more similarly to Pt and Fe than to Au and Ag or CoN₄ and NiN₄ (i.e., more close to a 4-electron catalyst than to a 2-electron catalyst) and therefore their activity moves toward the apex in a theoretical volcano correlation (see **Graphical Abstract**).

Electrochemical Characterization

Figures 5A–C illustrate a series of cyclic voltammograms measured at different scan rates (from 25 mV s^{-1} to 200 mV s^{-1}) of graphite electrodes modified with CoN₄-Py-CNT in N₂ saturated 0.1 M NaOH solutions. The intensity of the anodic peaks is directly proportional to the scan rate velocity as expected for surface defined redox processes. Generally, CoN₄ show an evident redox peak corresponding to the Co(II)/Co(I) transition at negative potentials (-0.715 V 8(2-Et-C₆H₁₁O)CoPc, -0.575 V for CoPc, -0.4 V vs. Ag/AgCl for 16(F)CoPc), while the redox potential for the Co(III)/(II) redox peak is less evident (Barrera et al., 2006; Hebié et al., 2016; Venegasa et al., 2017). For 8(2-Et-C₆H₁₁O)CoPc-Py-CNT the redox peak for Co(II)/Co(I) is not well defined and appears at a potential of $\approx -0.73 \text{ V}$ (**Figure 5A**). For the CoPc-Py-CNT complex the Co(II)/Co(I) is very well defined at a potential of $\approx -0.58 \text{ V}$ (**Figure 5B**). 16(F)CoPc-Py-CNT showed a not well defined redox peak at $\approx -0.5 \text{ V}$ (**Figure 5C**). Apparently, for this complex, the Py back ligand

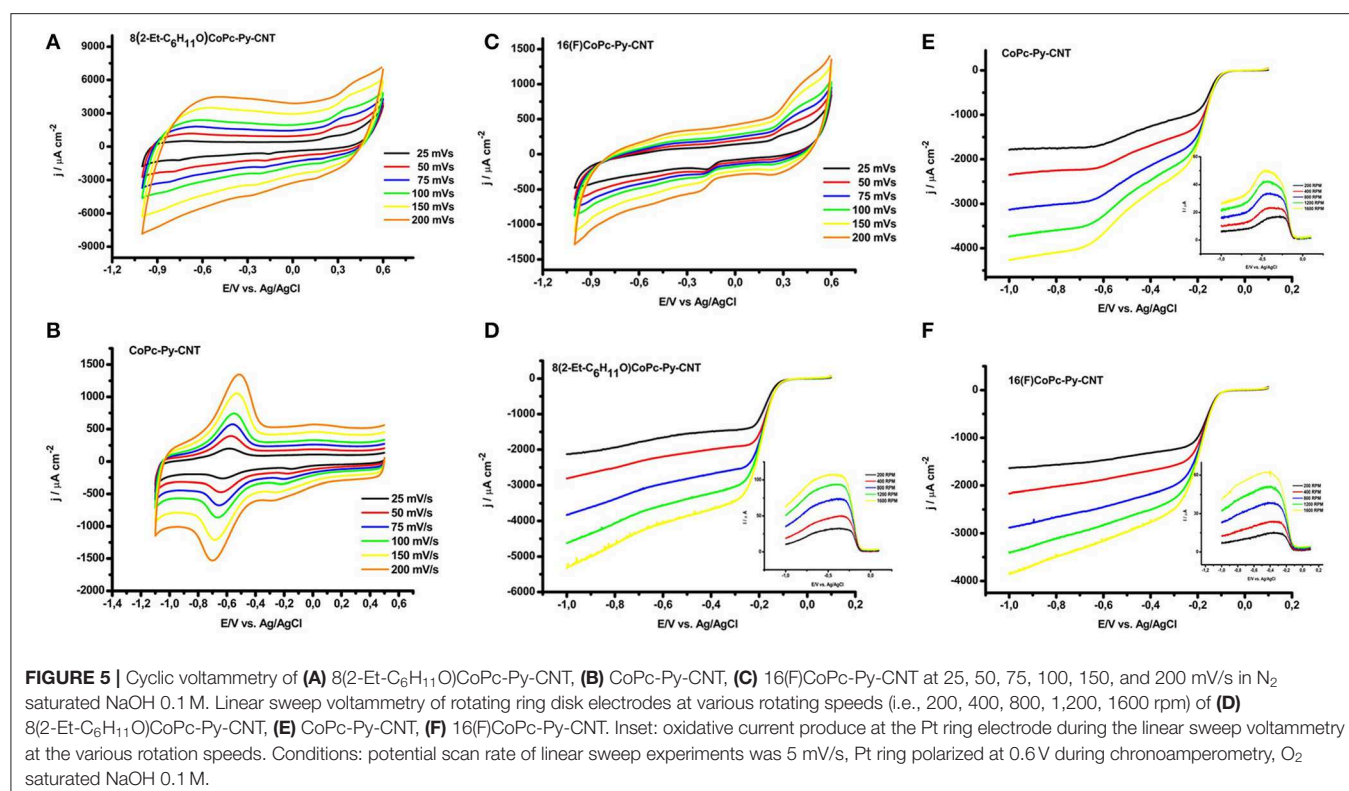


FIGURE 5 | Cyclic voltammetry of **(A)** 8(2-Et-C₆H₁₁O)CoPc-Py-CNT, **(B)** CoPc-Py-CNT, **(C)** 16(F)CoPc-Py-CNT at 25, 50, 75, 100, 150, and 200 mV/s in N₂ saturated NaOH 0.1 M. Linear sweep voltammetry of rotating ring disk electrodes at various rotating speeds (i.e., 200, 400, 800, 1,200, 1,600 rpm) of **(D)** 8(2-Et-C₆H₁₁O)CoPc-Py-CNT, **(E)** CoPc-Py-CNT, **(F)** 16(F)CoPc-Py-CNT. Inset: oxidative current produced at the Pt ring electrode during the linear sweep voltammetry at the various rotation speeds. Conditions: potential scan rate of linear sweep experiments was 5 mV/s, Pt ring polarized at 0.6 V during chronoamperometry, O₂ saturated NaOH 0.1 M.

TABLE 3 | Summary of the electrochemical results obtained for 8(2-Et-C₆H₁₁O)CoPc-Py-CNT (Blue), CoPc-Py-CNT (Black), and 16(F)CoPc-Py-CNT.

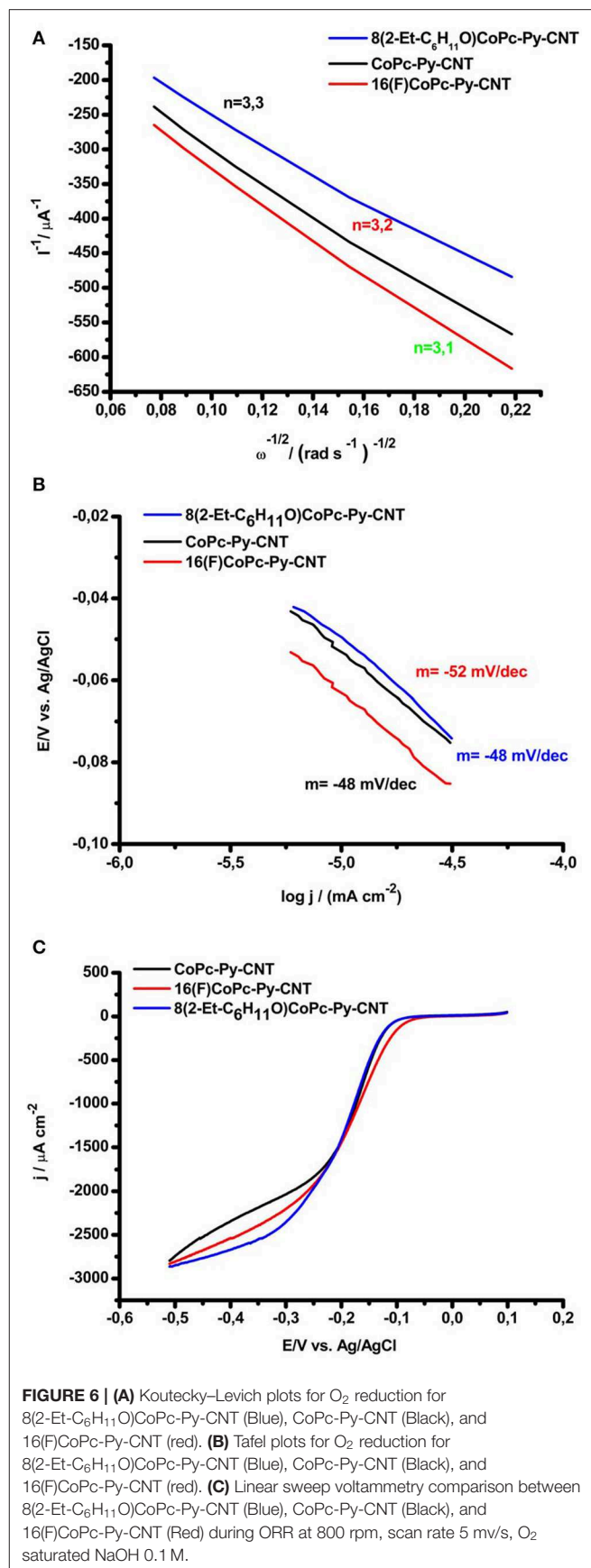
	Onset (V)	N e-measured at -0.5 V	Tafel Slope (V/decade)	E(Co(II)/I) (V)	Coverage (mol/cm ²)	TOF (S ⁻¹)
8(2-Et-C ₆ H ₁₁ O)CoPc-Py-CNT	-0.07	3.3	-0.052	-0.73	2.94×10^{-9}	0.4
CoPc-Py-CNT	0.07	3.2	-0.048	-0.58	1.52×10^{-9}	0.4
16(F)CoPc-Py-CNT	-0.05	3.1	-0.048	-0.50	5.57×10^{-10}	0.5

Onset for the ORR; number of electrons transferred during the ORR; Tafel slope; Co(II)/I formal potential; concentration of the complex determined by the integration of the redox peaks of the Co(II)/I redox couples; turn over frequency (TOF) for the complex during ORR.

acts as an electron-donating group. This might be an effect of the F groups located on the Pc ligand that essentially withdraw electron density from the axial Py group. These observations indicate that the combined electronic effects of the ligand and back ligand on the Co center are not additive, and are essentially push-pull electronic effects. Therefore, the effect of the axial coordination is opposite for the complexes with residues that are neutral or with a small electron-donating character and for the complex with a strong electron withdrawing residue as the perfluorinated compound. In **Table 3** we display the Co(II)/(I) redox peak potentials for the various CoN5 as well as the surface concentration of the catalysts obtained from the integration of the Co(II)/(I) redox oxidation peaks from **Figures 5A–C**.

In **Figures 5D–F**, we report the polarization curves for the ORR for electrodes modified with CoN5 in a 0.1 M NaOH solution saturated with O₂ at various rotation speeds (from 200 to 1600 rpm). The HO₂[−] produced during the ORR at CoN5 modified graphite disks was monitored by polarizing the Pt ring electrode mounted in the same shuffle of the disk at 0.6 V (insets of **Figures 5D–F**). The onset for the ORR starts around −0.07 V for 8(2-Et-C₆H₁₁O)CoPc-Py-CNT and CoPc-Py-CNT while it starts around −0.05 V for 16(F)CoPc-Py-CNT. The production of HO₂[−] follows similar trends to the ORR (i.e., it decreases as the ORR catalytic current increases). At low overpotentials, in the mixed mass transport and kinetic controlled region, high amounts of HO₂[−] were produced with a maximum at −0.35 V for both 8(2-Et-C₆H₁₁O)CoPc-Py-CNT and 16(F)CoPc-Py-CNT. The CoPc-Py-CNT follows a slightly different process with a more pronounced HO₂[−] production with a peak at −0.3 and a dramatic decrease at −0.5 V. Anyway, the three catalysts present a bell shaped curve for HO₂[−] production, but for the CoPc-Py-CNT catalyst the difference between the activities of Co(I) and Co(II) toward the ORR is more pronounced probably because in the absence of residues at the periphery the differences between Co(I) and Co(II) are more accentuated.

In **Figure 6A**, the extrapolation of the experimental Koutecky–Levich (K–L) plots are presented. The values were extrapolated at −0.750 V. This potential was chosen for comparison reason, whereas the n of electrons would decrease at lower overpotentials (e.g., −0.3 V), where higher amounts of HO₂[−] are produced. The Koutecky–Levich regression shows that the reduction at CoN5 involves approximately 3.2 electrons (values for the 3 complexes are resumed in **Table 3**), which is in contrast to the typical 2-electron reduction process generally reported for Co attached directly to graphite and in the absence of an axial ligand. It should be noted that at higher overpotential the HO₂ produced at the electrode surface decreases. This also suggests that the mechanism for the ORR is different from the CoN4. In **Figure 6B** the Tafel plots for the ORR for the CoN5 complexes are shown. The slopes determined from experiments presented values ranging from −0.048 V decade^{−1} to −0.052 V decade^{−1}. For CoN4, slopes in the range of −0.060 V decade^{−1} were obtained (Zagal and Koper, 2016; Venegasa et al., 2017). Slopes close to −0.060 V as for CoN4 complexes suggest that the first step involves a fast electron transfer followed by a slow rate determining chemical step. In contrast, slopes of −0.040 V



indicate that the first step involves a fast one-electron transfer followed by a slow one-electron transfer step. Generally slopes of -0.040 V are reported for Fe catalysts (Zagal and Koper, 2016; Venegasa et al., 2017). Slopes of ≈ -0.050 V decade $^{-1}$ would, therefore, represent a situation in the middle where a mixed behavior is expected. Similar values were obtained before for VB12 adsorbed on CNT (Riquelme et al., 2018a). In **Figure 6C** we report, for comparison, the linear sweep voltammetry during ORR for the three complexes at the same rotation speed (i.e., 800 rpm) and at the same conditions. The onset for the ORR is very similar for the three complexes ranging from -0.07 V to -0.05 V. The mass transport limiting catalytic current is reached already at -0.3 V, showing the similarities between the three complexes when in the presence of the pyridine axial ligand.

In **Table 3** we resume the turn over frequencies (TOF) estimated for CoN5 from the mass-related kinetic current density at -0.05 V. The comparison of the 3 TOF values reveals the similarity of the CoN5, which all can reduce O₂ at very similar velocities. The fifth N coordination appears to play a strong role in the activities of CoN5. The effect of the axial coordination is stronger than the effect of the same plane residues that can be attached to the molecule. Therefore, the 3 complexes studied in this work, show similar activities toward the ORR and similar TOF values and energy binding values.

In a previous publication, we reported that the presence of the pyridine axial ligand as in CoPc-Py-CNT or as in VB12 increases the Co-O₂ binding energy moving these complexes to the left-hand side of a volcano correlation, to the region of stronger M-O₂ binding energy (Zagal and Koper, 2016; Riquelme et al., 2018a). New calculations performed on both CoN5 and CoN4 show that this is not completely true. If we consider the activities for CoN4 published in Zagal and Koper (2016), Venegasa et al. (2017) and we correlate them with the calculated O₂ binding energy we can derive a linear correlation belonging to one side of a volcano correlation (Zagal and Koper, 2016). Also Zhou and collaborators showed an incremented activity toward the ORR increasing the electro-withdrawing force of the axial ligand coordinated to Co porphyrins (Zhou et al., 2019). This correlation would also be linear (i.e., only in one side the volcano). When in the presence of the back bond ligand Co phthalocyanines would bind O₂ stronger and therefore the increment in the catalytic activities. CoN5 complexes would then move toward the apex of the volcano if compared to CoN4. Nevertheless, this would not be sufficient for correlating the complexes with the strong binding side of the volcano (see **Graphical Abstract**).

REFERENCES

- Abarca, G., Viera, M., Aliaga, C., and Marco, J. F. (2019). In search of the most active MN4 catalyst for the oxygen reduction reaction. The case of perfluorinated Fe phthalocyanine. *J. Mat. Chem. A*, 7, 24776–24783. doi: 10.1039/C9TA09125D
- Assour, J. M. (1965). Solvent effects on the spin resonance spectra of cobalt phthalocyanine. *J. Am. Chem. Soc.* 87, 4701–4706. doi: 10.1021/ja00949a008

CONCLUSIONS

We report for the first time the EPR and XPS spectra of the penta-coordinated complexes 8(2-Et-C₆H₁₁O)CoPc-Py-CNT, CoPc-Py-CNT, and 16(F)CoPc-Py-CNT. For 8(2-Et-C₆H₁₁O)CoPc-Py-CNT, EPR and XPS spectra show that the metal center is Co(II) high spin ($S = 3/2$) species, while for CoPc-Py-CNT it is Co(II) in a low spin configuration $S = 1/2$. For 16(F)CoPc-Py-CNT an intermediate spin ($S = 1$) Co(III) species are more probable. O₂ binding energy were calculated and resulted to be very similar for the three complexes with values ranging from -0.52 to -0.59 eV. The CoN5 complexes were electrochemically characterized and their electrocatalytic activities toward the ORR were studied. Results show that the three complexes perform the ORR very similarly with a total of ≈ 3.2 electrons and Tafel slopes of ≈ -0.050 V decade $^{-1}$. Therefore, CoN5 have a mixed behavior between a 2 and a 4-electron catalyst for the ORR. The pyridine back ligand act as an electron-withdrawing group for 8(2-Et-C₆H₁₁O)CoPc-Py-CNT and CoPc-Py-CNT, but as an electron-donating group for 16(F)CoPc because of the presence of the F residues located on the phthalocyanine ligand. Therefore, the combined electronic effects of the ligand and back ligand on the Co center are essentially push-pull electronic effects.

DATA AVAILABILITY STATEMENT

The datasets generated for this study are available on request to the corresponding author.

AUTHOR CONTRIBUTIONS

MV and JR performed electrochemical experiments. CA performed EPR experiments. JM performed XPS experiments. WO performed DFT calculation. JZ supervised the experimental and writing session. FT provided the main idea, writing, and supervision of the entire work.

ACKNOWLEDGMENTS

FT thanks for financial support the Fondecyt Project 1181840, and Proyecto Basale Dicyt. JZ thanks for the financial support of Millenium Project RC120001, Project Anillo ACT 1412 and Dicyt-USACH, Fondecyt 1140199. WO thanks for the financial support from Fondecyt Project 1170480 and Powered@NLHPC for the supercomputing infrastructure of the NLHPC (ECM-02). The authors acknowledge the laboratory of free radicals for the use of the EPR (USACH) and CONICYT-FONDEQUIEQM140060.

- Bahr, J. L., and Tour, J. M. (2001). Highly functionalized carbon nanotubes using *in situ* generated diazonium compounds. *Chem. Mater.* 13, 3823–3824. doi: 10.1021/cm0109903
- Barrera, C., Zhukov, I., Villagra, E., and Bedioui, F. (2006). Trends in reactivity of unsubstituted and substituted cobalt-phthalocyanines for the electrocatalysis of glucose oxidation. *J. Electroanal. Chem.* 589, 212–218. doi: 10.1016/j.jelechem.2006.02.009

- Baumgarten, M., Winscom, C. J., and Lubitz, W. (2001). Probing the surrounding of a cobalt(II) porphyrin and its superoxo complex by EPR techniques. *App. Magn. Res.* 20, 35–70. doi: 10.1007/BF03162310
- Bedioui, F., Griveau, S., Nyokong, T., Appleby, A. J., Caro, C. A., Gulppi, M., et al. (2007). Tuning the redox properties of metalloporphyrin and metallophthalocyanine-based molecular electrodes for the highest electrocatalytic activity in the oxidation of thiols. *Phys. Chem. Chem. Phys.* 9, 3383–3396. doi: 10.1039/b618767f
- Berland, K., Cooper, V. R., Lee, K., Schröder, E., Thonhauser, T., Hyldgaard, P., et al. (2015). van der Waals forces in density functional theory: a review of the vdW-DF method. *Rep. Prog. Phys.* 78:066501. doi: 10.1088/0034-4885/78/6/066501
- Briggs, D., and Gibson, V. A. (1974). Direct observation of multiplet splitting in 2P photoelectron peaks of cobalt complexes. *Chem. Phys. Lett.* 25, 493–496. doi: 10.1016/0009-2614(74)85350-9
- Cariati, F., Galizzioli, D., Morazzoni, F., and Busetto, C. (1975). New adducts of (phthalocyaninato)cobalt(II) with pyridine and 4-methylpyridine and their vibrational, magnetic, and electronic properties. I. Reactivity towards oxygen. *J. Chem. Soc., Dalton Trans.* 556–561. doi: 10.1039/dt9750000556
- Christensen, R., Hansen, H. A., Dickens, C. F., Nørskov, J. K., and Vegge, T. (2016). Functional independent scaling relation for ORR/OER catalysts. *J. Phys. Chem. C* 120, 24910–24916. doi: 10.1021/acs.jpcc.6b09141
- Collman, J. P., Denisevich, P., Konai, Y., Marrocco, M., Koval, C., and Anson, F. C. (1980). Electrode catalysis of the four-electron reduction of oxygen to water by dicobalt face-to-face porphyrins. *J. Am. Chem. Soc.* 102, 6027–6036. doi: 10.1021/ja00539a009
- Corzilius, B., Dinse, K. P., and Hata, K. (2007). Single-wall carbon nanotubes and peapods investigated by EPR. *Phys. Chem. Chem. Phys.* 9, 6063–6072. doi: 10.1039/b707936m
- Dey, S., Mondal, B., Chatterjee, S., Rana, A., Amanullah, S., and Dey, A. (2017). Molecular electrocatalysts for the oxygen reduction reaction. *Nat. Rev. Chem.* 1:0098. doi: 10.1038/s41570-017-0098
- Durand, R. R. Jr., Bencosme, C. S., Collman, J. P., and Anson, F. C. (1983). Mechanistic aspects of the catalytic reduction of dioxygen by cofacial metalloporphyrins. *J. Am. Chem. Soc.* 105, 2710–2718. doi: 10.1021/ja00347a032
- Frost, D. C., McDowell, C. A., and Woolsey, I. S. (1974). X-ray photoelectron spectra of cobalt compounds. *Molecular Phys.* 6, 1473–1489. doi: 10.1080/00268977400101251
- Fukuzumi, S., Lee, Y.-M., and Nam, W. (2018). Mechanisms of two-electron versus four-electron reduction of dioxygen catalyzed by earth-abundant metal complexes. *ChemCatChem* 10, 9–28. doi: 10.1002/cctc.201701064
- Garrity, K. F., Bennett, J. W., Rabe, K. M., and Vanderbilt, D. (2014). Pseudopotentials for high-throughput DFT calculations. *Comp. Mat. Sci.* 81, 446–452. doi: 10.1016/j.commatsci.2013.08.053
- Geraldo, D., Linares, C., Chen, Y.-Y., Ureta-Zañartu, S., Zagal, J. H. (2002). Volcano correlations between formal potential and Hammett parameters of substituted cobalt phthalocyanines and their activity for hydrazine electro-oxidation. *Electrochem. Comm.* 4, 182–187. doi: 10.1016/S1388-2481(01)00300-9
- Geraldo, D. A., Togo, C. A., Limson, J., Nyokong, T. (2008). Electrooxidation of hydrazine catalyzed by noncovalently functionalized single-walled carbon nanotubes with CoPc. *Electrochim. Acta.* 53, 8051–8057. doi: 10.1016/j.electacta.2008.05.083
- Giannozzi, P., Baroni, S., Bonini, N., Calandra, M., Car, R., Cavazzoni, C., et al. (2009). Quantum Espresso: a modular and open-source software project for quantum simulations of materials. *J. Phys. Condens. Mat.* 21:395502. doi: 10.1088/0953-8984/21/39/395502
- Gulppi, M. A., Recio, F. J., Tasca, F., and Ochoa, G. (2014). Optimizing the reactivity of surface confined cobalt N4-macrocyclics for the electrocatalytic oxidation of L-cysteine by tuning the Co(II)/(I) formal potential of the catalyst. *Electrochim. Acta.* 126, 37–41. doi: 10.1016/j.electacta.2013.07.230
- Hansen, H. A., Viswanathan, V., and Nørskov, J. K. (2014). Unifying kinetic and thermodynamic analysis of 2 e- and 4 e- reduction of oxygen on metal surfaces. *J. Phys. Chem. C* 118, 6706–6718. doi: 10.1021/jp4100608
- Hebié, S., Bayo-Bangoura, M., Bayo, K., Servat, K., Morais, C., Napporn, T. W., et al. (2016). Electrocatalytic activity of carbon-supported metallophthalocyanine catalysts toward oxygen reduction reaction in alkaline solution. *J. Solid State Electrochem.* 20, 931–942. doi: 10.1007/s10008-015-2932-6
- Henkelman, G., Uberuaga, B. P., and Jonsson, H. A. (2000). A climbing image nudged elastic band method for finding saddle points and minimum energy paths. *J. Chem. Phys.* 113, 9901–9904. doi: 10.1063/1.1329672
- Herrera, S., Tasca, F., Williams, F. J., and Calvo, E. J. (2018). Adsorption of 4,4-dithiodipyridine axially coordinated to iron (II) phthalocyanine on Au (111) as a new strategy for oxygen reduction electrocatalysis. *ChemPhysChem.* 19, 1599–1604. doi: 10.1002/cphc.201800139
- Jasinski, R. (1964). A new fuel cell cathode catalyst. *Nature* 201, 1212–1213. doi: 10.1038/2011212a0
- Katsounaros, I., and Koper, M. T. M. (2017). “Electrocatalysis for the hydrogen economy,” in *Electrochemical Science for a Sustainable Society: A Tribute to John O’M Bockris*, ed K. Uosaki (Cham: Springer International Publishing), 23–50. doi: 10.1007/978-3-319-57310-6-2
- Kontarinis, D., Paraskevas, S. M., and Paraskevas, M. S. (2003). Oxygen adducts of Co-phthalocyanine, synthesis and reactivity in inorganic and metal-organic. *Chemistry.* 33, 1381–1389. doi: 10.1081/SIM-120024316
- Koper, M. T. M. (2011). Thermodynamic theory of multi-electron transfer reactions: implications for electrocatalysis. *J. Electroanal. Chem.* 660, 254–260. doi: 10.1016/j.jelechem.2010.10.004
- Le Mest, Y., Inisan, C., Laouenan, A., L’Her, M., Talarmin, J., El Khalifa, M., et al. (1997). Reactivity toward dioxygen of dicobalt face-to-face diporphyrins in aprotic media. Experimental and theoretical aspects. possible mechanistic implication in the reduction of dioxygen. *J. Am. Chem. Soc.* 119, 6095–6106. doi: 10.1021/ja9618659
- Liao, M.-S., and Scheiner, S. (2001). Electronic structure and bonding in metal phthalocyanines, Metal = Fe, Co, Ni, Cu, Zn, Mg. *J. Chem. Phys.* 114, 9780–9791. doi: 10.1063/1.1367374
- Linares-Flores, C., Mac-Leod Carey, D., Muñoz-Castro, A., Zagal, J. H., Pavez, J., Pino-Riffo, D., et al. (2012). Reinterpreting the role of the catalyst formal potential. the case of thiocyanate electrooxidation catalyzed by CoN4-macrocyclic complexes. *J. Phys. Chem. C* 116, 7091–7098. doi: 10.1021/jp300764n
- Menanteau, T., Dias, M., Levillain, E., Downard, A. J., and Breton, T. (2016). Electrografting via diazonium chemistry: key role of aryl substituent in layer growth mechanism. *J. Phys. Chem. C* 120, 4423–4429. doi: 10.1021/acs.jpcc.5b12565
- Morlanes, N., Takanabe, K., and Rodionov, V. (2016). Simultaneous reduction of CO₂ and splitting of H₂O by a single immobilized cobalt phthalocyanine electrocatalyst. *ACS Catal.* 6, 3092–3095. doi: 10.1021/acscatal.6b00543
- Nørskov, J. K., Rossmeisl, J., Logadottir, A., Lindqvist, L., Kitchin, J. R., and Bligaard, T., et al. (2004). Origin of the overpotential for oxygen reduction at a fuel-cell cathode. *J. Phys. Chem. B* 108, 17886–17892. doi: 10.1021/jp047349j
- Oku, M. (1978). X-ray photoelectron spectrum of low-spin Co(III) in LiCoO₂. *J. Solid State Chem.* 23, 177–185. doi: 10.1016/0022-4596(78)90063-4
- Oldacre, A. N., Crawley, M. R., Friedman, A. E., and Cook, T. R. (2018). Tuning the activity of heterogeneous cofacial cobalt porphyrins for oxygen reduction electrocatalysis through self-assembly. *Chem. Eur. J.* 24, 10984–10987. doi: 10.1002/chem.201802585
- Orellana, W. (2012). Metal-phthalocyanine functionalized carbon nanotubes as catalyst for the oxygen reduction reaction: a theoretical study. *Chem. Phys. Lett.* 541, 81–84. doi: 10.1016/j.cplett.2012.05.048
- Orellana, W. (2013). Catalytic properties of transition metal-N4 moieties in graphene for the oxygen reduction reaction: evidence of spin-dependent mechanisms. *J. Phys. Chem. C* 117, 9812–9818. doi: 10.1021/jp4002115
- Peljo, P., Murtomäki, L., Kallio, T., Xu, H. J., Meyer, M., Gros, C. P., et al. (2012). Biomimetic oxygen reduction by cofacial porphyrins at a liquid-liquid interface. *J. Am. Chem. Soc.* 134, 5974–5984. doi: 10.1021/ja3004914
- Riquelme, J., Neira, K., Marco, J. F., Hermosilla, P., Venegas, D., Orellana, W., et al. (2018b). Climbing over the activity volcano correlation by biomimicking vitamin B12: a Co phthalocyanine pyridine axial ligand coordinated catalyst for the reduction of molecular oxygen. *ECS Transac.* 85, 111–121. doi: 10.1149/08512.0111ecst
- Riquelme, J., Neira, K., Marco, J. F., Hermosilla-Ibáñez, P., Orellana, W., Zagal, J. H., et al. (2018a). Biomimicking vitamin B12. A Co phthalocyanine pyridine axial ligand coordinated catalyst for the oxygen reduction reaction. *Electrochim. Acta.* 265, 547–555. doi: 10.1016/j.electacta.2018.01.177

- Ruiz-Tagle, I., and Orellana, W. (2010). Iron porphyrin attached to single-walled carbon nanotubes: electronic and dynamical properties from *ab initio* calculations. *Phys. Rev. B Condens. Matter Mater. Phys.* 82, 115401–115406. doi: 10.1103/PhysRevB.82.115406
- Steiger, B., and Anson, F. C. (1995). Evidence of the importance of back-bonding in determining the behavior of ruthenated cyanophenyl cobalt porphyrins as electrocatalysts for the reduction of dioxygen. *Inorg. Chem.* 34, 3355–3357. doi: 10.1021/ic00116a031
- Sun, B., Ou, Z., Meng, D., Fang, Y., Song, Y., Zhu, W., et al. (2014). Electrochemistry and catalytic properties for dioxygen reduction using ferrocene-substituted cobalt porphyrins. *Inorg. Chem.* 53, 8600–8609. doi: 10.1021/ic501210t
- Swavey, S., and Eder, A. (2013). Enhanced O₂ electrocatalysis by a highly conjugated cobalt(II) porphyrin. *Inorg. Chem. Commun.* 29, 14–17. doi: 10.1016/j.inoche.2012.11.028
- Tasca, F., Harreither, W., Ludwig, R., Gooding, J. J., and Gorton, L. (2011). Cellobiose dehydrogenase Aryl diazonium modified single walled carbon nanotubes: enhanced direct electron transfer through a positively charged surface. *Anal. Chem.* 83, 3042–3049. doi: 10.1021/ac103250b
- Tse, Y.-H., Janda, P., Lam, H., Zhang, J., Pietro, W. J., and Lever, A. B. P. (1997). Monomeric and polymeric tetraaminophthalocyaninatocobalt(II) modified electrodes: electrocatalytic reduction of oxygen. *J. Porph. Phthaloc.* 1, 3–16.
- Tuci, G., Zafferoni, C., Rossin, A., Milella, A., Luconi, L., Innocenti, M., et al. (2014). Chemically functionalized carbon nanotubes with pyridine groups as easily tunable N-decorated nanomaterials for the oxygen reduction reaction in alkaline medium. *Chem. Mater.* 26, 3460–3470. doi: 10.1021/cm500805c
- Van Den Brink, F., Visscher, W., and Barendrecht, E. (1983). Electrocatalysis of cathodic oxygen reduction by metal phthalocyanines: part Introduction I cobalt phthalocyanine as electrocatalyst: experimental part. *J. Electroanal. Chem. Interf. Electrochem.* 157, 283–304. doi: 10.1016/0022-0728(83)80335-0
- Venegas, R., Javier Recio, F., Riquelme, J., and Neira, K. (2017). Biomimetic reduction of O₂ in acid medium on iron phthalocyanines axially coordinated to pyridine anchored on carbon nanotubes. *J. Mat. Chem. A.* 5, 12054–12059. doi: 10.1039/C7TA02381B
- Venegas, R., Recio, J. F., Zuñiga, C., Viera, M., Oyarzún, M. P., Silva, N., et al. (2017). Comparison of the catalytic activity for the reduction of O₂ of Fe and Co MN4 complexes adsorbed on the edge plane graphite electrodes and on carbon nanotubes. *Phys. Chem. Chem. Phys.* 19, 20441–20450. doi: 10.1039/C7CP03172F
- Viswanathan, V., Hansen, H. A., Rossmesl, J., and Nørskov, J. K. (2012). Unifying the 2e- and 4e- reduction of oxygen on metal surfaces. *J. Phys. Chem. Lett.* 3, 2948–2951. doi: 10.1021/jz301476w
- Wada, T., Maki, H., Imamoto, T., Yuki, H., and Miyazato, Y. (2013). Four-electron reduction of dioxygen catalyzed by dinuclear cobalt complexes bridged by bis(terpyridyl)anthracene. *Chem. Commun.* 49, 4394–4396. doi: 10.1039/C2CC36528F
- Weber, J. H., and Busch, D. H. (1965). Complexes derived from strong field ligands. XX. The effect of extraplanar ligands on the properties of transition metal 4,4',4''-tetrasulfophthalocyanines. *Inorg. Chem.* 4, 472–475. doi: 10.1021/ic50026a008
- Ye, L., Fang, Y., Ou, Z., Xue, S., and Kadish, K. M. (2017). Cobalt tetrabutano- and tetrabenzotetraarylporphyrin complexes: effect of substituents on the electrochemical properties and catalytic activity of oxygen reduction reactions. *Inorg. Chem.* 56, 13613–13626. doi: 10.1021/acs.inorgchem.7b02405
- Zagal, J., Paez, M., Tanaka, A. A., and Linkous, C. A. (1992). Electrocatalytic activity of metal phthalocyanines for oxygen reduction. *J. Electroanal. Chem.* 339, 13–30. doi: 10.1016/0022-0728(92)80442-7
- Zagal, J. H., Griveau, S., Silva, J. F., Nyokong, T., and Bedioui, F. (2010). Metallophthalocyanine-based molecular materials as catalysts for electrochemical reactions. *Coord. Chem. Rev.* 254, 2755–2791. doi: 10.1016/j.ccr.2010.05.001
- Zagal, J. H., and Koper, M. T. M. (2016). Reactivity descriptors for the activity of molecular MN4 catalysts for the oxygen reduction reaction, *Angew. Chem. Internat. Ed.* 55, 14510–14521. doi: 10.1002/anie.201604311
- Zhang, X., Wu, Z., Zhang, X., Li, L., Li, Y., Xu, H., et al. (2017). Highly selective and active CO₂ reduction electrocatalysts based on cobalt phthalocyanine/carbon nanotube hybrid structures. *Nat. Comm.* 8:14675. doi: 10.1038/ncomms14675
- Zhou, Y., Xing, Y. F., Wen, J., Ma, H. B., Wang, F. B., and Xia, X. H. (2019). Axial ligands tailoring the ORR activity of cobalt porphyrin. *Sci. Bull.* 64, 1158–1166. doi: 10.1016/j.scib.2019.07.003

Conflict of Interest: The authors declare that the research was conducted in the absence of any commercial or financial relationships that could be construed as a potential conflict of interest.

Copyright © 2020 Viera, Riquelme, Aliaga, Marco, Orellana, Zagal and Tasca. This is an open-access article distributed under the terms of the Creative Commons Attribution License (CC BY). The use, distribution or reproduction in other forums is permitted, provided the original author(s) and the copyright owner(s) are credited and that the original publication in this journal is cited, in accordance with accepted academic practice. No use, distribution or reproduction is permitted which does not comply with these terms.